High contrast ballistic imaging using a femtosecond optical Kerr gate of $SrTiO_3$ crystal

2013 Laser Phys. Lett. 10 055407

(http://iopscience.iop.org/1612-202X/10/5/055407)

IOP PUBLISHING LASER PHYSICS LETTERS
Laser Phys. Lett. **10** (2013) 055407 (5pp) doi:10.1088/1612-2011/10/5/055407

LETTER

High contrast ballistic imaging using a femtosecond optical Kerr gate of $SrTiO_3$ crystal

Bin Wu[1], Wenjiang Tan[1], Xin Liu[2], Jinhai Si[1], Pingping Zhan[1], Lihe Yan[1], Feng Chen[1] and Xun Hou[1]

[1] Key Laboratory for Physical Electronics and Devices of the Ministry of Education and Shaanxi Key Lab of Information Photonic Technique, School of Electronic and Information Engineering, Xi'an Jiaotong University, Xianning-xilu 28, Xi'an 710049, People's Republic of China
[2] Science and Technology on Electro-Optical Information Security Control Laboratory, Sanhe 065201, People's Republic of China

E-mail: jinhaisi@mail.xjtu.edu.cn

Received 1 October 2012
Accepted for publication 17 January 2013
Published 3 April 2013
Online at stacks.iop.org/LPL/10/055407

Abstract
We investigated a ballistic imaging technique using a femtosecond optical Kerr gate (OKG) made of $SrTiO_3$ crystal (STO). High-contrast images of a 1.41 line pairs per mm (lp mm^{-1}) section of the resolution test chart placed behind a turbid medium were obtained. The STO OKG had greater capacity to acquire high quality images at a high optical density than the quartz OKG, showing that the STO is a promising OKG medium due to its large nonlinear susceptibility.

(Some figures may appear in colour only in the online journal)

1. Introduction

With the widespread use of femtosecond lasers, ballistic imaging has become an active field of study because of its potential applications in medical diagnosis [1] and fluid dynamics measurement [2]. A critical problem in ballistic imaging is that the majority photons of the beam suffer scattering in highly turbid media and these photons will lead to a blurring of the image. So the essence of this imaging technique is to separate the unscattered photons (also known as ballistic photons or signal photons) from the multiply scattered photons (also known as diffusive photons or noise photons). An obvious technique appears to be time gating, which exploits the fact that the scattered photons arrive at the detector later than the ballistic photons. Therefore, using appropriate time gating techniques, image-bearing photons can be picked out. In this decade, many systems have taken advantage of time gating to mitigate scattered light by using the ultrafast optical Kerr gate (OKG) technique [2–4]. The OKG technique has been used to investigate the dynamics of spray breakup and vaporization in the near field of the liquid-fueled combustion of a high-speed rocket spray by measuring the velocity and acceleration vectors that describe the forces active in primary breakup [4–7].

The performance of an OKG is strongly affected by the Kerr medium. A suitable Kerr medium should have large nonlinearity, ultrafast response time and a wide transparent window. In previous typical applications of the OKG technique [8–12], CS_2 and fused quartz were used. CS_2 possess large nonlinear susceptibility, but has a nonlinear response time of ∼2 ps [13], which originates from molecular reorientation. So the molecular reorientation time limits the

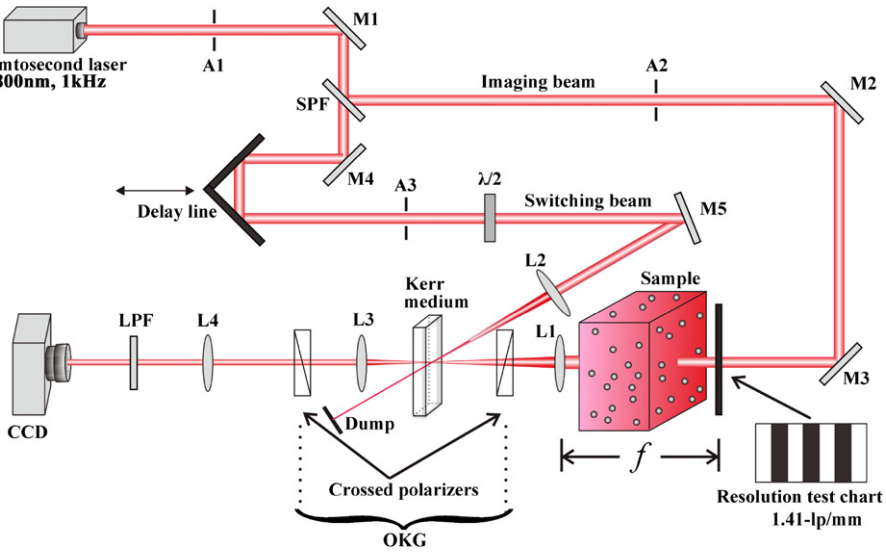

Figure 1. Schematic of the ballistic imaging system: L, lens; M, mirror; $\lambda/2$, half wave plate; A, aperture; SPF, short pass filter; LPF, long pass filter.

switch time. The fused quartz has wide transmittance over a wide spectral range, but its nonlinear susceptibility is low. Over the last few decades, great efforts have been made in the research and development of nonlinear optical materials [14–16]. $SrTiO_3$ crystal (STO) is a promising transparent material and has a good lattice match to most materials with the perovskite structure, and has been widely used in special optical windows and high quality sputtering targets [17, 18]. The nonlinear response of STO originates from electronic processes, and the nonlinear refractive index is estimated to be 2.16×10^{-15} cm^2 W^{-1} [19]. As the STO crystal has good nonlinear optical properties, it may be attractive in the application of the OKG technique in the future.

In this paper, we investigated ballistic imaging based on OKGs made from STO and quartz, respectively. Images of a resolution test chart placed behind a turbid medium were obtained by testing a series of samples with different optical densities (ODs). Compared with the quartz OKG, the STO OKG had greater capacity to acquire high quality images at a high optical density due to the larger nonlinear susceptibility of STO.

2. Experiments

A schematic of the ballistic imaging system in our experiments is shown in figure 1. A Ti:sapphire laser system with a repetition rate of 1 kHz and a pulse duration of 50 fs at 800 nm was employed. The output of the pulsed beam was split into two beams using a short pass filter (SPF). The high power beam was used as the imaging beam, and it was modulated by a 1.41 line pairs per mm (1 p mm^{-1}) section of the resolution test pattern (a United States Air Force contrast target) which was placed on the conjugate imaging plane of the CCD camera. The transmitted scattered light from the sample was collected by a lens (L1) which was placed one focal distance from the resolution test pattern, and then it passed through an ultrafast OKG. The OKG was structured by a pair of crossed Nicol polarizers which bracket a Kerr medium, and it was gated by the switching beam with low power. This beam was time delayed by an adjustable-length delay line and then was rotated 45° by a half-wave plate for maximum gate efficiency. The Kerr signal was subsequently collected by two lenses (L3, L4) and directed to a CCD camera (Nikon DXM 1200F). A long pass filter (LPF) was placed between a lens (L4) and the camera in order to decrease the intensity of the noise generated by the pump scattering in the Kerr medium, which was the main source of noise in these experiments. By this system, the ballistic light, which traveled a shorter path than the scattered light, reached the Kerr medium first and could be effectively picked out temporally by the OKG.

In order to preferentially gate the image-bearing part of the transmitted light, the optical delay line was adjusted so that the switch pulse temporally overlaps with the image-bearing part of the transmitted pulse. This process was facilitated by first optimizing the imaging beam passing through the sample cuvette filled with water instead of the scattering sample. It ensures the temporal overlap between the switching pulse and the image-bearing part of the transmitted pulse in the presence of the scattering sample. At this optimum delay, the image of the resolution test chart was detected on the CCD. So the image consists of a high-resolution and high-contrast projection of the resolution test chart.

In the experiment, the samples filled in the cuvette (10 mm thick) were monodisperse suspensions of polystyrene microspheres with a mean diameter of 0.4 m in water. The different ODs were controlled by the concentrations of polystyrene microspheres in water. The STO and the quartz were both 1 mm thick.

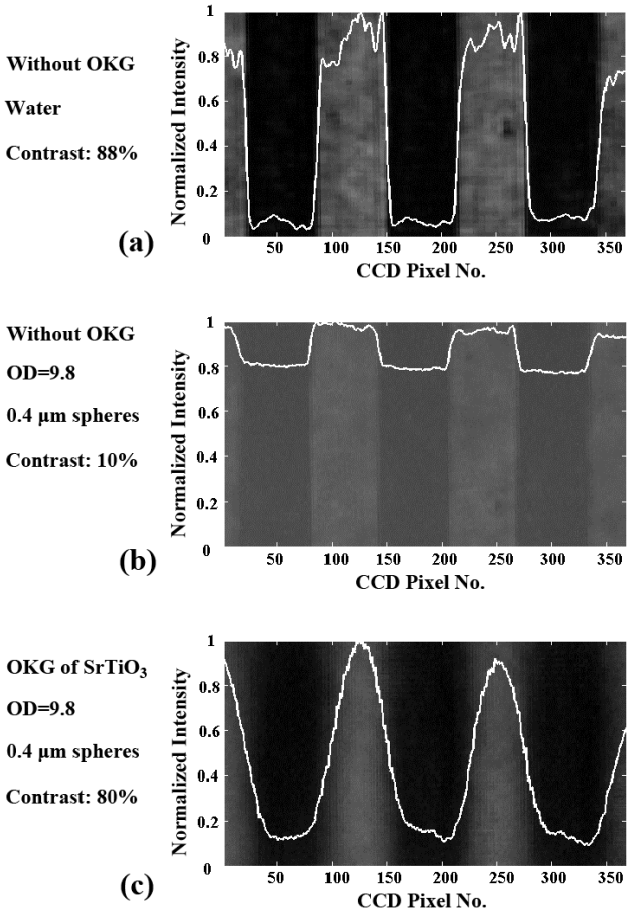

Figure 2. Comparison of the image contrast and the intensity: (a) through water and without the OKG; (b) through scattering sample and without the OKG; (c) through scattering sample and with the STO OKG. Results are shown together with the corresponding plots of one-dimensional (summed) intensity versus CCD pixel number for the conditions listed on the left.

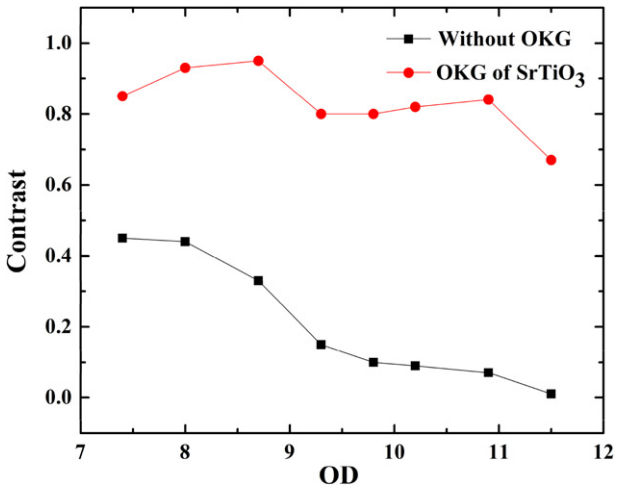

Figure 3. Comparison of the image contrast with and without an OKG, at ODs of 7.4, 8.0, 8.7, 9.3, 9.8, 10.2, 10.9 and 11.5.

3. Results and discussion

3.1. Enhancing the image contrast via the OKG

An essential aspect of an optical system is its ability to transmit spatial information. The relevant parameter for evaluating performance in this respect is the visibility, or image contrast, of the image. Contrast is given as

$$\text{Contrast} = \frac{I_{\max} - I_{\min}}{I_{\max} + I_{\min}} \tag{1}$$

where $I_{\min}$ is the average light intensity corresponding to the shaded region and $I_{\max}$ is the average light intensity corresponding to the unshaded region of the imaged resolution test chart.

The 1.41 p mm^{-1} section of the resolution test chart was selected as the imaging object. First we obtained the image of the resolution test chart under the condition of filling the sample cuvette with distilled water and without the OKG, as shown in figure 2(a), and the corresponding plots of one-dimensional intensity versus CCD pixel number are shown together with the image. The contrast calculated by equation (1) was 88%. We regarded this image as the original image of the imaging object. Then, we acquired the image under the condition of filling the sample cuvette with the polystyrene sphere solution and without the OKG. As shown in figure 2(b), we acquired this image at OD 9.8, and the contrast of this image was 10%. Finally, using the STO OKG, we acquired the image under the condition of filling the sample cuvette with the polystyrene sphere solution. As shown in figure 2(c), this image was obtained at the same OD as figure 2(b), but the contrast of this image has been enhanced to 80%. By comparing figure 2(a) with figure 2(b) we found that the contrast of the image was evidently decreased via scattering. From figures 2(c) and (b) we found the contrast of the image had been greatly enhanced by the STO OKG. It should be noted that the sharpness of the boundaries is decreased via the OKG imaging system. As our optical configuration was originally adapted from the 'Kerr–Fourier' imaging setup in [20], this phenomenon can be well understood according to the spatial filtering effect.

Then we measured the different images at different ODs of 7.4, 8.0, 8.7, 9.3, 9.8, 10.2, 10.9 and 11.5 by varying the concentration of the polystyrene sphere solution, and we obtained images at every OD with and without the STO OKG. We calculated the contrast of all the images by equation (1). When there is no OKG we can clearly see that the contrast of the images decreases rapidly from 0.45 to 0.01 with the increase in OD in figure 3. The contrast of images obtained by the STO OKG fluctuates at a range of 0.67–0.95 when the OD changes. For a given OD, the contrast of images obtained by the OKG is obviously higher than the contrast of images obtained for the situation of without the OKG because the OKG effectively eliminates the scattered light which will deteriorate image contrast. These results strongly indicate that the OKG is a very useful tool for eliminating noise and enhancing image contrast.

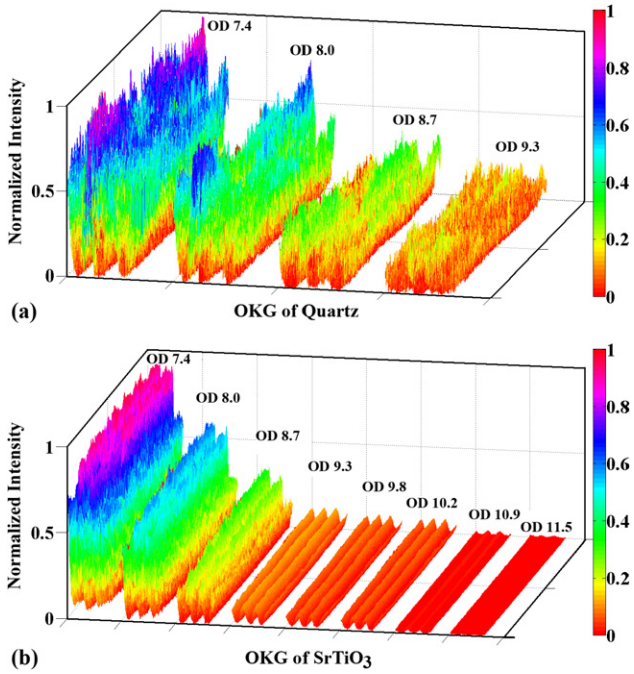

Figure 4. Two-dimensional spatial intensity distributions of the images obtained by two OKGs at different ODs: (a) quartz OKG; (b) STO OKG.

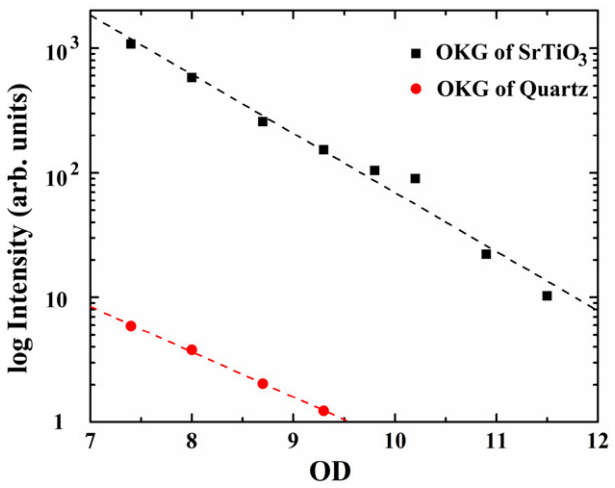

Figure 5. The intensities obtained by the two OKGs at different ODs.

3.2. The performance comparison of different OKGs in ballistic imaging

In a further experiment, we compared the ballistic imaging using the STO and quartz OKGs.

Figure 4 shows the two-dimensional spatial intensity distributions of the images when STO and quartz were used as Kerr media, respectively. In this measurement, a series of scattering samples with ODs of 7.4, 8.0, 8.7, 9.3, 9.8, 10.2, 10.9 and 11.5 were used. Using the quartz OKG, recognizable images can be obtained at ODs of 7.4, 8.0, 8.7 and 9.3, as shown in figure 4(a). When the OD increased more, recognizable images could not be obtained by the quartz OKG in experiments, but for the STO OKG, clear and recognizable images could still be acquired even at OD 11.5, as shown in figure 3(b). Furthermore, the shaded regions and the unshaded regions of the images obtained by the quartz OKG could not be identified clearly, and so many intensity glitches emerge in these regions at ODs 7.4, 8.0, 8.7 and 9.3, as shown in figure 3(a). However, the shaded and the unshaded regions were distributed uniformly in the images obtained by the STO OKG at all the ODs, which could be recognized easily.

The intensities of the Kerr signals obtained by the STO and quartz OKGs are shown in figure 5. We can see there is a good linear relationship between the logarithm of intensity and the OD. This relationship conforms well to Beer's law and demonstrates that the intensity of the two group images in figure 4 decreases exponentially with the increase in OD, indicating that scattered light was isolated efficiently by the OKG and the rest of the transmitted light was almost all ballistic light. We can also find that the transmitted intensity obtained by the STO OKG is larger than the transmitted intensity obtained by the quartz OKG at the same ODs, which can be attributed to the high third-order nonlinear susceptibility of STO. These results indicated that the STO OKG had superiority in ballistic imaging compared to the quartz OKG.

4. Conclusion

In summary, using STO and quartz OKGs in a ballistic imaging technique we obtained images of a 1.41 p mm^{-1} section of the resolution test chart placed behind turbid media at a series of ODs. Our studies showed that both the quality and the intensity of the images obtained by the STO OKG were higher than those obtained by the quartz OKG at the same OD. STO crystal has been demonstrated to be a promising OKG medium due to its ultrafast response time and large nonlinear susceptibility, and it may be attractive for application of the OKG technique in the future.

Acknowledgments

The authors gratefully acknowledge the support from the National Science Foundation of China under the grant nos 61235003, 61205129 and 91123028, the Natural Science Basic Research Plan in Shaanxi Province of China (program no. 2012JQ8002), the Eyas Project of the Academy of Opto-Electronics of Chinese Academy of Sciences and the Fundamental Research Funds for the Central Universities.

References

[1] Wang L, Ho P P, Liu C, Zhang G and Alfano R R 1991 *Science* **253** 769–71
[2] Linne M, Paciaroni M, Berrocal E and Sedarsky D 2009 *Proc. Combust. Inst.* **32** 2147–61
[3] Tong J Y, Yang Y, Si J H, Tan W J, Chen F, Yi W H and Hou X 2011 *Opt. Eng.* **50** 043607
[4] Paciaroni M and Linne M 2004 *Appl. Opt.* **43** 5100–9

[5] Paciaroni M, Linne M, Hall T, Delplanque J P and Parker T 2006 *Atomization Sprays* **16** 51–69
[6] Schmidt J B, Schaefer Z D, Meyer T R, Roy S, Danczyk S A and Gord J R 2009 *Appl. Opt.* **48** B137–44
[7] Sedarsky D, Gord J, Carter C, Meyer T and Linne M 2009 *Opt. Lett.* **34** 2748–50
[8] d'Abzac F X, Kervella M, Hespel L and Dartigalongue T 2012 *Opt. Express* **20** 9604–15
[9] Tamayo-Rivera L, Rangel-Rojo R, Mao Y and Watson W H 2008 *Opt. Commun.* **281** 5239–43
[10] Falcao E L, Bosco C A C, Maciel G S, de Araujo C B, Acioli L H, Nalin M and Messaddeq Y 2003 *Appl. Phys. Lett.* **83** 1292–4
[11] Symes D R, Wegner U, Ahlswede H C, Streeter M J V, Gallegos P L, Divall E J, Smith R A, Rajeev P P and Neely D 2010 *Appl. Phys. Lett.* **96** 011109
[12] Ma C S, Kwok W M, Chan W S, Zuo P, Kan J T W, Toy P H and Phillips D L 2005 *J. Am. Chem. Soc.* **127** 1463–72
[13] Sala K and Richardson M C 1975 *Phys. Rev.* A **12** 1036–47
[14] Tan W J, Liu H, Si J H and Hou X 2008 *Appl. Phys. Lett.* **93** 0511095
[15] Liu Y, Qin F, Wei Z Y, Meng Q B, Zhang D Z and Li Z Y 2009 *Appl. Phys. Lett.* **95** 131116
[16] Guo H T, Hou C Q, Gao F, Lin A X, Wang P F, Zhou Z G, Lu M, Wei W and Peng B 2010 *Opt. Express* **18** 23275–84
[17] Rouèdea D, Le Granda Y, Leroya L, Duclèreb J R and Guilloux-Viryb M 2003 *Opt. Commun.* **222** 289–97
[18] Kan D S *et al* 2005 *Nature Mater.* **4** 816–9
[19] Yan L H, Jia S, Si J H, Matsuo S, Chen F and Hou X 2012 *Chin. Phys. Lett.* **29** 074207
[20] Wang L, Ho P P, Liang X, Dai H and Alfano R R 1993 *Opt. Lett.* **18** 241–3